Fachtagung "Experimentelle Strömungsmechanik"
7.–9. September 2021, Bremen

Ein neuartiges Modellexperiment zur Untersuchung der Oberflächen- strukturen in Wechselwirkung mit einem Überschallgasstrahl

A new liquid metal experiment to investigate surface wave behaviour in a BOF converter

Johannes Burkert, Rüdiger Schwarze

Institut für Mechanik und Fluiddynamik, TU Bergakademie Freiberg Lampadiusstraße 4, 09599 Freiberg, Deutschland Johannes.Burkert@imfd.tu-freiberg.de

Oberflächenwellen, Wechselwirkung freie Oberfläche-Gasstrahl

Surface waves, top blown jet, interaction liquid surface-gas jet

Summary

The time-resolved measurement of surface structures and waves, which are formed by the impact of a gas jet, is of high relevance from a technical as well as from a flow-physical point of view. In this paper, a novel experimental setup is presented, which allows to investigate and characterize such structures experimentally by optical and non-invasive measurement methods (see Figure 1). The results allow first conclusions on the correlation between nozzle height, surface patterns and wave propagation frequency. With increasing nozzle height, the formation of ripple waves increases, as the frequency spectrum between suggests.

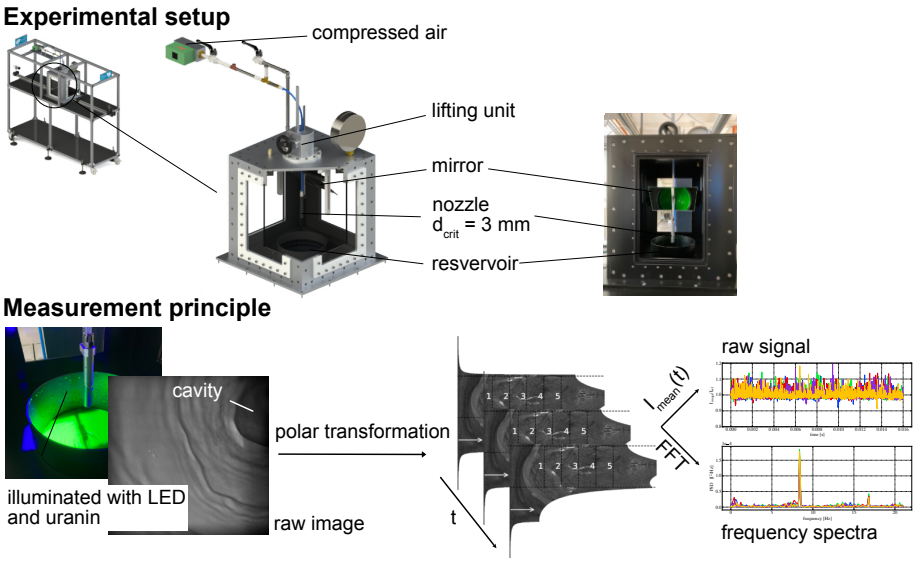

Figure 1:Graphical summary of the experimental setup and the measurement principle for the investigation of the surface structures.

Introduction

The interaction of supersonic gas jets and a free liquid or solid surface is of technical as well as fluid-physical importance. For example, this process is used in the Blast Oxygen Furnace, BOF for short, for steel production (Peaslee and Robertson, 1994) in surface finishing with paints (Muñoz-Esparza et al., 2012) or in vertically taking off jet aircraft, so-called VTOL, (Kumar et al., 2013). The underlying fluid mechanics is therefore of high importance in order to optimize these processes. For the BOF process, a large number of experimental studies have investigated the formation of a so-called cavity in the impact region of the gas jet. It was shown that, depending on the nozzle height and gas jet impulse, the formation of the cavity can be divided into three regimes: Wave formation, spattering and penetration.

In this context, extensive measurements have been made in Banks and Chandrasekhara, 1963, Cheslak et al., 1969, Molloy, 1970, Evestedt and Medvedev, 2005 and He and Belmonte, 2010 to name a few parameters such as nozzle height above the surface, supplied volumetric flow rate and incident angle of the gas jet. Experiments were performed in a water-oil emulsion or with flash concrete. Ek and Du Sichen, 2012 also investigated cavity behavior, but used the liquid metal alloy Gallinstan (Ga-In-Sn) as the experimental fluid for the first time. Further, an oscillation of the cavity is observed, which was mentioned by Molloy, 1970 but not described further. Further, Evestedt and Medvedev, 2005 and He and Belmonte, 2010 give a frequency range between 2 and 20 Hz, but in both papers the cause of the oscillation is not discussed further. Gelderloos, Juni/2010 described in a similar model experiment a frequency spectrum in the range 0 to 50 Hz and pointed out that structures in the gas jet significantly influence the cavity oscillation.

In addition to the above-mentioned experimental work, the problem has recently been investigated by numerical studies. Works by Asahara et al., 2011 and Kalifa et al., 2020 showed that the gas jet is reflected back in the cavity and emerges at the cavity walls. Depending on the magnitude of the gas jet momentum, flow separation and breakaway of individual droplets occurs. If the gas jet impulse is low, the gas jet runs parallel to the surface and generates ripple-like surface waves.

The short overview of the literature shows that the behaviour of the cavity and the liquid surface has been extensively studied, but without including the gas jet itself. However, the works of Mendez et al., 2018 and Mendez et al., 2019 suggest that the understanding of the gas jet dynamics is of great importance for the behaviour of the surface waves as well as the cavity is essential. In addition, most of the aforementioned work was performed in 2D experiments, which neglects the three-dimensional behaviour of the surface. To fill this gap, a novel model experiment is presented in the present work, which investigates the surface waves in a three-dimensional container using optical non-invasive methods. In addition, the gas jet can also be studied optically to obtain a more detailed understanding of the interaction between the gas jet and the surface.

Experimental Setup

In the following section, the basic setup of the test rig is described, and the optical measurement method is presented. The core of the test rig is the measuring chamber (Figure 2 a)), which provides optical access from four sides. The chamber mainly consists of the compressed air supply, the nozzle lifting unit, the mirror system, the nozzle and the cylindrical liquid reservoir ($d_R = 200\,mm$). The nozzle height can be varied with the lifting unit between

GALA e.V., Karlsruhe, Germany, ISBN 978-3-9816764-7-1

$h_{nozzle} = 100\,mm$ and $h_{nozzle} = 200$ above the liquid surface. The maximum possible filling level of the reservoir is $h_{Fluid} = 100\,mm$. The compressed air is provided by the laboratory's own compressed air supply and has a maximum pressure difference of $8\,bar$ against atmosphere. The nozzle has a critical diameter of $d_{krit} = 3\,mm$ which theoretically allows a maximum Mach number of 3. All components are made of stainless steel or powder coated to avoid a reaction with the liquid model melt Galinstan® used later.

Figure 2 b) shows the measurement principle used to detect the surface waves. The mirrors are used to observe the surface waves without optical distortion through the viewing windows. The light loss due to the mirrors is compensated by using high power LEDs. The camera LED and camera are placed side by side so that the LED is oriented at a small angle to the camera.

In the preliminary tests with water as model liquid, the upstream pressure difference was initially limited to a maximum of $\Delta p_{in} = 0.4\,bar, 0.6\,bar\ and\ 0.8\,bar$, since a clear droplet and spray formation was already evident here. The tests only serve to check the measuring principle for the later tests with Galinstan®. The nozzle height was varied out between $h_{nozzle} = 40\,mm$ und $h_{nozzle} = 200\,mm$ in intervals of $\Delta h_{nozzle} = 20\,mm$. The acquisition frequency of the camera was set to $f_S = 42\,Hz$ with each measurement series consisting of 1000 individual images. The images are recorded with a colour depth of $16\,bit$ to obtain the highest possible information content. For the measurements a *Pointgrey Grashopper 3* with a maximum resolution of $2048\,x\,2048\,pixel$ was used. In combination with a field of view width of 100 mm this leads to a pixel scale of $20.48\,pixel/mm$.

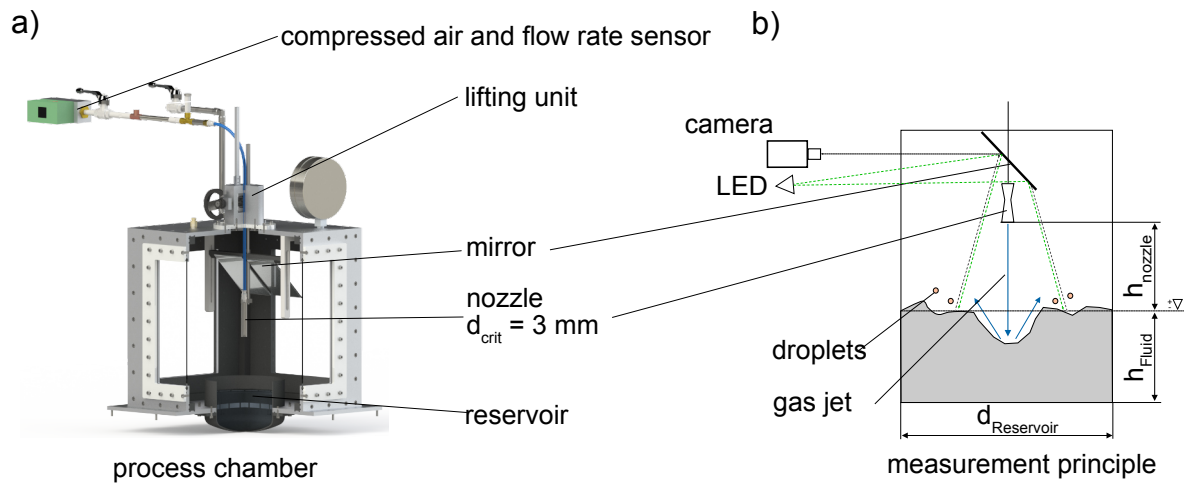

Figure 2: a) CAD model of the measuring chamber. b) Representation of the measuring principle with the relevant geometric quantities

In addition, the test rig is equipped with a Schlieren imaging setup to optically detect the gas jet structures above the liquid surface. For this approach two achromatic lenses with a focal length $f_{focal} = 1000\,mm$ and $d_{lens} = 100\,mm$ are used to provide a high sensitivity of the system. Since the gas jet has highly transient structures a pulsed LED is in use for illumination. So, this setup in combination with a *Phantom V12* ($1280\,x\,800\,pixel$) high speed camera enables time resolved measurements of the gas jet itself. This allows us to observe and describe the relationship between the gas jet and the surface waves in more detail. The optical setup is displayed in Figure 3. Since, the initial measurements are performed at subcritical pressures the Schlieren imaging is not used here so far. However, the gas jet structures are the scope of the future measurements.

GALA e.V., Karlsruhe, Germany, ISBN 978-3-9816764-7-1

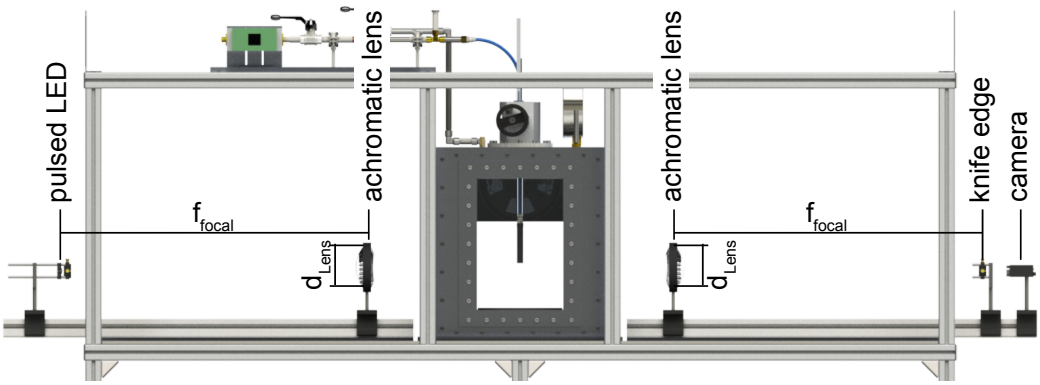

Figure 3: Schlieren imaging setup to characterize the gas jet structures.

Data Processing

The evaluation is done in several steps with the freely available image processing library *OpenCV* in combination with *Python 3.8*. The general procedure is shown in the following Figure 4. The raw images are first histogram adjusted to normalize the gray values. Then an image crop is performed followed by the determination of the impact point of the gas jet. In the next step, the image is polar transformed around this point. This results in a transformed image with only one direction of propagation, in this case from left to right. The radial propagation of the waves is thus transformed into a linear motion, which simplifies the subsequent evaluation.

The transformed images are now used to characterize the frequency spectra of the wave propagation. For this purpose, the pixel intensities at five different radial positions are extracted. For each line and time step the average value is calculated to avoid a position dependence of the measured data. For a Fast Fourier Transformation (FFT) it is generally recommended to use integral quantities. However, since these are not available, the mean values of the pixel intensities per time step are used. The FFT is performed with the function *scipy.signalwelch()* in Python. For a better evaluation of the signal a Blackman windowing and a signal segmentation into 512 segments is given.

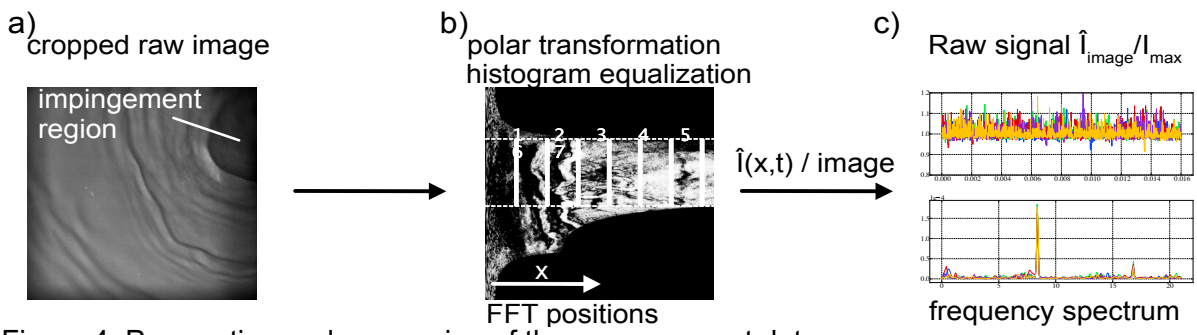

Figure 4: Preparation and processing of the measurement data

The data processing of the Schlieren imaging is done the same way but without the polar transformation.

Results and Discussion

The results of the preliminary tests are shown in the following figures Figure 5 and Figure 6. Figure 5 shows instantaneous snapshots of the measurements. The cavity is marked with a dotted circle. The penetrating, splashing and dimple mode can be clearly seen for the differ-

ent parameters and are marked with solid lined circles. Droplet separation for the penetrating and splashing mode are also visible. Interestingly, the droplets also generate surface waves when they fall back into the liquid bath (marked as secondary waves in Figure 5 b)). These the interact with the surface waves created by the gas jet. However, we were not able to get clear images for $h_{nozzle} = 40 - 120\,mm$ for $\Delta p_{in} = 0.6bar$ respectively $\Delta p_{in} = 0.8bar$ due to the high droplet generation and splashing. Both lead to a blocked view on the mirror. The further away the nozzle is from the surface, the lower the impulse input because the gas jet becomes continuously wider.

As a result, the impact region is flatter but also wider, which means that the gas jet tends to sweep over the surface, leading to the formation of ripple waves on the surface. The ripple waves are represented by a broad background noise in the frequency spectrum, which occurs from a nozzle height of $120\,mm$ to $180\,mm$, depending on the upstream pressure. Previous work from the study of wind induced waves confirms this assumption Mitsuyasu and Honda, 1974;and 1974, Mataoui et al., 2003. Ripple waves appear here in the form of broadly distributed frequencies with low energy content. These waves occur primarily when wind passes over the water surface and energy exchange occurs between the air and the water surface.

The further away the nozzle is from the surface, the lower the impulse input because the gas jet becomes continuously wider. As a result, the impact region is flatter but also wider, which means that the gas jet tends to sweep over the surface, leading to the formation of ripple waves on the surface. The ripple waves are represented by a broad background noise in the frequency spectrum, which occurs from a nozzle height of $120\,mm$ to $180\,mm$, depending on the upstream pressure. Previous work from the study of wind induced waves confirms this assumption Mitsuyasu and Honda, 1974; 1974, Mataoui et al., 2003. Ripple waves appear here in the form of broadly distributed frequencies with low energy content. These waves occur primarily when wind passes over the water surface and energy exchange occurs between the air and the water surface.

Samples of the frequency analysis are shown in Figure 6. Each spectrum shows a dominant frequency at $8\,Hz$ and $16\,Hz$, which is largely consistent with the works of Evestedt and Medvedev, 2005 and Li et al., 2019. Both give a frequency spectrum for the cavity between 0 and $20\,Hz$. These frequencies are more dominant the closer the nozzle and thus the higher the momentum transmitted by the gas jet. As a result, the cavity becomes deeper and has a smaller diameter (see Figure 5 a) and b)). It is known from the literature that the gas flows out of the cavity along the walls over the edges and that individual droplets break off as Figure 5 confirms for $p_{in} = 0.4\,bar$ and $40 - 120\,mm$ and $p_{in} = 0.6\,bar$ and $80 - 160\,mm$ and $p_{in} = 0.8\,bar$ and $160\,mm$.This behaviour is visible by the smaller frequency peaks around the two dominant frequencies

Conclusion

Our results show that we are able to detect the time resolved surface wave propagations in dependency of the nozzle height and the pressure difference in a three-dimensional measurement approach which is a clear advantage over previous works. The scope of upcoming measurements will be the use of Galinstan® as a liquid model melt to achieve a closer understanding of the surface wave propagation of molten steel.

GALA e.V., Karlsruhe, Germany, ISBN 978-3-9816764-7-1

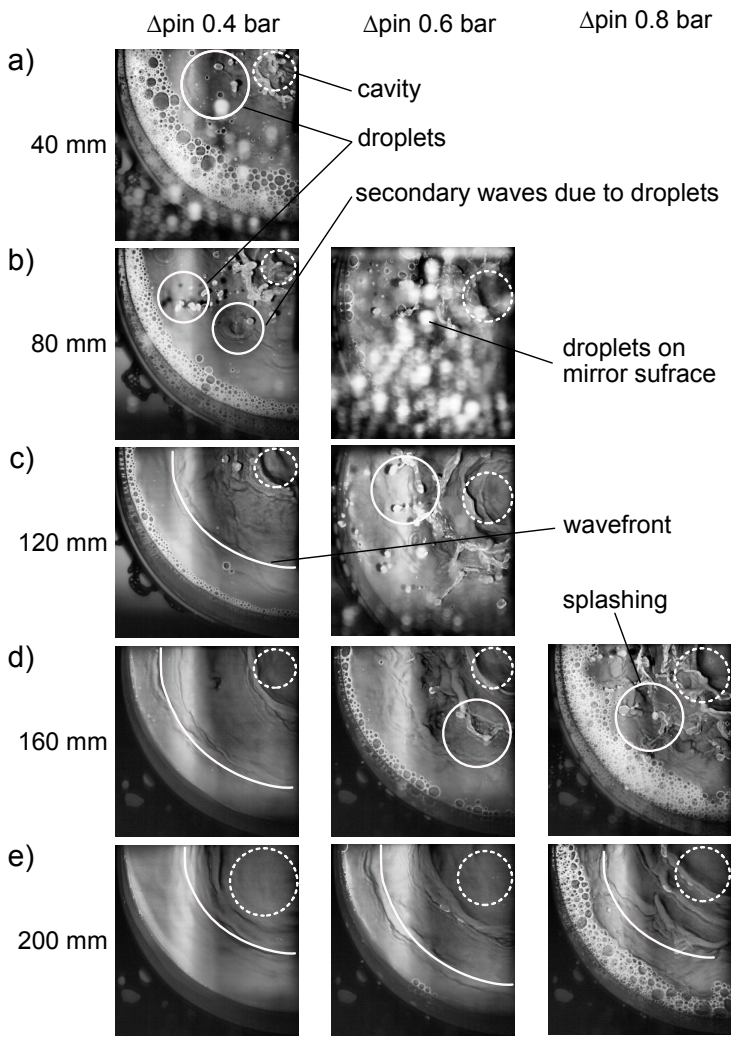

Figure 5: Instantaneous snapshots and phenotypical results of the initial measurements

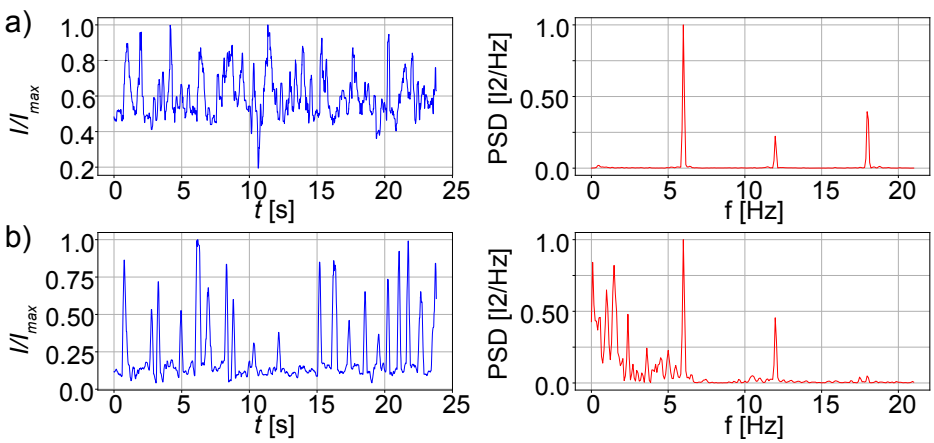

Figure 6: Sample of the frequency analysis of the surface wave propagation for a) $40\ mm$ and b) $200\ mm$ both at $\Delta p_{in} = 0.4\ bar$.

Acknowledgement

We thank the German Research Foundation for funding this project (SCHW1168/15-1). We also thank Mr. Kevin Schulze for helpful discussions regarding the design and manufacturing of the test rig and to Mr. Lukas Jung, who assisted the measurements.

Literature

Asahara, N., Naito, K. I., Kitagawa, I., Matsuo, M., Kumakura, M. and Iwasaki, M. (2011). Fundamental study on interaction between top blown jet and liquid bath. *Steel Research International*. **82**, 587–594. doi:10.1002/srin.201100041.

Banks, R. and Chandrasekhara, D. (1963). Experimental investigation of the penetration of a high-velocity gas jet through a liquid surface. *Journal of Fluid Mechanics*. **15**, 13–34.

Cheslak, F., Nicholls, J. and Sichel, M. (1969). Cavities formed on liquid surfaces by impinging gaseous jets. *Journal of Fluid Mechanics*. **36**, 55–63.

Ek, M. and Du Sichen (2012). Study of penetration depth and droplet behavior in the case of a gas jet impinging on the surface of molten metal using liquid Ga-In-Sn. *Steel Research International*. **83**, 678–685. doi:10.1002/srin.201100336.

Evestedt, M. and Medvedev, A. (2005). Gas jet impinging on liquid surface: Cavity shape modelling and video-based estimation. *14746670*. **16**. doi:10.3182/20050703-6-cz-1902.00178.

Gelderloos, R. (Juni/2010). Dynamics of Air-Blown Dimples.

He, A. and Belmonte, A. (2010). Deformation of a liquid surface due to an impinging gas jet: A conformal mapping approach. *Physics of Fluids*. **22**, 1–7. doi:10.1063/1.3327209.

Kalifa, R. B., Hamza, S. B., Saïd, N. M. and Bournot, H. (2020). Fluid flow phenomena in metals processing operations: Numerical description of the fluid flow field by an impinging gas jet on a liquid surface. *International Journal of Mechanical Sciences*. **165**, 105220. doi:10.1016/j.ijmecsci.2019.105220.

Kumar, R., Wiley, A., Venkatakrishnan, L. and Alvi, F. (2013). Role of coherent structures in supersonic impinging jets. *Physics of Fluids*. **25**, 76101. doi:10.1063/1.4811401.

Li, M., Li, Q., Zou, Z. and Li, B. (2019). Characterization of Cavity Oscillation and Splashing Distribution Under Excitation by Bottom Gas Blowing in a Steelmaking Converter. *Jom*. **71**, 729–736. doi:10.1007/s11837-018-3203-7.

Mataoui, A., Schiestel, R. and Salem, A. (2003). Study of the oscillatory regime of a turbulent plane jet impinging in a rectangular cavity. *Applied Mathematical Modelling*. **27**, 89–114. doi:10.1016/S0307-904X(02)00050-1.

Mendez, M. A., Gosset, A. and Buchlin, J. M. (2019). Experimental analysis of the stability of the jet wiping process, part II: Multiscale modal analysis of the gas jet-liquid film interaction. *Experimental Thermal and Fluid Science*. **106**, 48–67. doi:10.1016/j.expthermflusci.2019.03.004.

Mendez, M. A., Scelzo, M. T. and Buchlin, J.-M. (2018). Multiscale modal analysis of an oscillating impinging gas jet. *Experimental Tehrmal and Fluid Science*. **91**, 256–276.

Mitsuyasu, H. and Honda, T. (1974). The high frequency spectrum of wind-generated waves. *Journal of the Oceanographical Society of Japan*. **30**, 185–198. doi:10.1007/BF02111070.

Molloy, N. A. (1970). Impinging Jet Flow in a Two-Phase System. The Basic Flow Pattern. *Journal of The Iron and Steel Institute*, 943–950.

Muñoz-Esparza, D., Buchlin, J. M., Myrillas, K. and Berger, R. (2012). Numerical investigation of impinging gas jets onto deformable liquid layers. *Applied Mathematical Modelling*. **36**, 2687–2700. doi:10.1016/j.apm.2011.09.052.

Peaslee, K. D. and Robertson, G. C. (1994). Fluid Dynamics of Inclined Jetting on a Slag-Metal Bath. In *TMS EPD Congress 1994, G.W. Warren, Editor, TMS, Warrendale, PA,* pp. 1129–1145.

GALA e.V., Karlsruhe, Germany, ISBN 978-3-9816764-7-1